How a colloidal paste flows
– scaling behaviors in dispersions of aggregated particles under mechanical stress –

R. Botet*, B. Cabane†, M. Clifton**, M. Meireles** and R. Seto*,‡

*Laboratoire de Physique des Solides, Université Paris-Sud, CNRS-UMR8502, Orsay F-91405, France
†Laboratoire PMMH, ESPCI, 10 Rue Vauquelin, Paris Cedex 05 F-75231, France
**Laboratoire de Génie Chimique, Université Paul Sabatier, CNRS-UMR5503, Toulouse F-31062, France
‡Department of Physics, Ritsumeikan University-BKC, Kusatsu City 525-8577, Japan

Abstract. We have developed a novel computational scheme that allows direct numerical simulation of the mechanical behavior of sticky granular matter under stress. We present here the general method, with particular emphasis on the particle features at the nanometric scale. It is demonstrated that, although sticky granular material is quite complex and is a good example of a challenging computational problem (it is a dynamical problem, with irreversibility, self-organization and dissipation), its main features may be reproduced on the basis of rather simple numerical model, and a small number of physical parameters. This allows precise analysis of the possible deformation processes in soft materials submitted to mechanical stress. This results in direct relationship between the macroscopic rheology of these pastes and local interactions between the particles.

INTRODUCTION

The case of sticky granular matter is far from new. It is defined as solid particles dispersed in a fluid phase, with hard-core and short-range attractive interaction between the particles. It includes such important topics as slurries [1], cements [2], ink [3], paints [4], all kind of pastes [5], sandcastles [6], or blood [7]. Last, they form the bulk of industrial and city effluents. Wet granular materials [8] form a generic class of sticky granular matter. The flow of these materials, when they are submitted to mechanical stress, is the most important issue common to all these examples.

An important point to notice, is that most of the particle interactions in the dense colloidal suspensions are noncentral forces, as they originate in surface interactions. This is worth recalling here that systems with central and noncentral forces may behave quite differently [10]. Moreover, these interactions are non-permanent, as they can be destroyed by stress. Material deformations are then irreversible and dissipative, what corresponds to a class of actual challenging computational problems.

Deformation of low volume fraction of dispersed particles is governed by particular scaling laws. This can be exemplified through an ideal gas of particles compressed under controlled energy. In this case, the Poisson's adiabatic law applies, namely :

$$P \propto \phi^{\gamma} , \qquad (1)$$

relating pressure P to volume fraction ϕ. The value of the adiabatic exponent γ is in the range $1.3 \sim 1.7$, depending on the way the gas particles reallocate energy.

A fractal aggregate in a fluid medium is an example of a non-ideal dispersion. The correlation length is then infinite, hence the system is at a critical point, and ϕ is the order parameter. Moreover, the thermodynamical field conjugated to the volume fraction is the external pressure. The general "magnetic" relation describing how the system loses criticality when a small field is applied, writes here as the scaling law :

$$P \propto \phi^{\delta} , \qquad (2)$$

with δ a critical exponent. This relation, deduced from the general theory of the critical phenomena, is formally similar to (1).

At last, for the highly concentrated solid particle dispersion in a continuous phase, the particles form complex disordered patterns and the forces propagate along particular paths - possibly fractal -, of connected particles. Therefore, response to external forces depend on the internal structure of the network made with the solid parts. Rheology of such strongly-flocculated dispersions is complex, and little is known about possible general laws relating stress and volume fraction [9].

The purpose of the present work is to discuss numerical models of disordered systems of hard particles interacting through noncentral, non-permanent, forces, and to

understand how such systems deform and flow when they are submitted to external stresses.

NUMERICAL MODEL

We will discuss the model as a system of hard particles embedded in the ordinary 3-dimensional continuous space [11]. It was also studied in the 2-dimensional space, as it may represent experimental situations as well (colloidal dispersions between glass plates [12]). Variants were considered to know which features of the model are relevant or not. They are briefly discussed below.

As a matter of fact, the basic model is issued from ideas of the discrete element method [13], used for granular matter modeling. Namely, each particle is regarded as an individual hard element and actual microscopic forces result from pair interaction. Hence, the solid phase is essentially granular matter, except that the interaction forces are *not* due to friction.

The dispersion.–

Basics.–

The incoming solid matter dispersed in the liquid consists in monodispersed hard spheres of radius a, and confined into a finite box, with periodic boundary conditions along two perpendicular directions, while fixed boundary conditions are used in the third direction.

Variants.–

Other convex particle shapes can be considered (e.g. platelets), with additional technical complications for the treatment of the possible overlaps. A simple way is to combine several spheres through unbreakable bonds in order to make individual particles of about the desired shape. In addition, the particles can be made rigid or deformable according to the stiffness (infinite or finite) of the permanent bonds.

Another point is polydisperse material. Tries with Gaussian distributions show that this is irrelevant for the constitutive equations. But more special distributions (e.g. Pareto distribution) have not been studied so far.

Of course, periodic boundary conditions can be replaced by fixed boundary conditions if needed (e.g. simulation of a colloidal paste between two plates).

The bonds.–

Basics.–

Short-range attractive interaction between the particles results from Van der Waals interactions, local chemical bonds (e.g. polycations), and screened electrostatic forces. Formation of such attractive bonds between the particles is modelled by creation of massless harmonic springs – whose stiffness is characteristic of the potential curvature of the interaction potential –, whenever the distance between two particle surfaces is less than the equilibrium value, l_o. This defines the energy unit E_o as the energy needed to compress the spring completely, as well as the pressure unit $P_o \equiv E_o/\pi a^3(l_o/2a)$. For E_o of order $1k_BT$ at room temperature, and a in the range $3 \sim 5$ nm, one obtains P_o of order 1 bar.

During rearrangement of the system, a spring may break whenever its length exceeds the threshold, l_{max}. Such breakable springs is the numerical materialization of the chemical bonds. The ratio between the energy of a spring at the rupture threshold and the energy to compress it completely (namely : $E_d/E_o = (l_{max}/l_o)^2 - 1$, which is called the reduced disruptive energy) is a fundamental non-dimensional parameter of the model.

Variants.–

Distribution of stiffness can be considered straightforwardly. This can be particularly important in the case where two or more different chemical counterions are used for flocculation.

Non-harmonic springs can be considered as well. But the relevant feature is the bottom of the attractive potential energy, therefore anharmonicity is not expected to play significant role.

Location of the bonds.–

Basics.–

In the real systems, the number of bonds between two particles is limited, either because the bonding energy is finite or because of excluded volume effect on the chemical bonds. We take this constraint into account by considering that springs can attach only at definite locations, called *pins*, on the surface of each particle. Only one bond can be attached to a given pin at the same time. The pins are defined randomly (with the uniform distribution) for each particle, once and for all at the beginning of each simulation. Consequently, each particle is entirely represented by the list of its pins
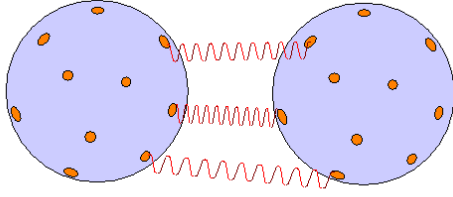
FIGURE 1. Schematic view of two spheres connected by a few springs. Pins are marked as small chips on the surface of each sphere. Two bonds cannot attach to the same pin, and a given bond connects two different spheres. Typically $200 - 500$ pins per particle surface are used.

(Fig.1), and its local frame which translates and rotates with respect to the overall reference frame of the box.

Variants.–

In some conditions, non-uniform spatial distribution of the pins can be considered. This could be the case for more complex geometries, for example with platelets for which one can clearly control the mechanism of aggregation through the distribution of the pins (e.g. pins localized on the largest faces of the platelets will result in stack arrangement, while 2-dimensional structures will appear if they are localized on the edges of the platelets).

Movement equations.–

Basics.–

When pressure is applied to the particle network, particles are submitted to the pressure forces, which, for spheres, are central in nature (contrary to the forces due to stretching of the bonds, which are essentially noncentral). In the frame of the box, the full equations of motion for the spherical particle i (radius a, mass m), submitted to force $\vec{F}_i$ and moment $\vec{M}_i$, are:

$$
\begin{aligned}
m\frac{d\vec{v}_i}{dt} &= \vec{F}_i + \lambda\left(\vec{v}_f - \vec{v}_i\right) , \\
\frac{5}{2}ma^2\frac{d\vec{\omega}_i}{dt} &= \vec{M}_i + \frac{4}{3}a^2\lambda\left(\vec{\omega}_f - \vec{\omega}_i\right) ,
\end{aligned}
\tag{3}
$$

where $\vec{v}_i$ and $\vec{\omega}_i$ denote the translational and angular velocity of the particle, and $\vec{v}_f, \vec{\omega}_f$ the corresponding macroscopic velocities of the fluid at the location of particle i. The coefficient λ is the proportionality constant between the drag force on a particle and its relative translational velocity with respect to the fluid in the Stokes regime.

In the present work, we will discuss only the quasi-static regime, *i.e.* the characteristic compression time is much larger than the relaxation time of the overall structure. Within such approximation, the system evolves through molecular dynamics (e.g. Verlet algorithm [14]), according to (3) where the drag forces are neglected. Pressure is then applied by small incremental steps, and mechanical relaxation of the structure is achieved before applying the next pressure step.

Variants.–

An alternative for the dynamics of such a system in the quasi-static regime, consists in replacing the classical equations (3) by a Monte Carlo procedure. In this approach, a particle of the system is chosen randomly. This particle is moved randomly (random translation + random rotation) if the change of energy is consistent with the Metropolis condition [14]. If the shift is effective, relaxation is performed, *i.e.* bonds are destroyed or created according to the rules governing the bonds. All this sequence is repeated until statistical equilibrium is reached.

Since the deformation process is governed by energies, one has to define forces through gradients. For example, the pressure force P is defined through the equation $\Delta E = -P\Delta H$, where ΔE is the difference of the system energy for a decrease ΔH of the system height. Note that the total system energy is the sum of the energies of all the bonds and of the energies previously released in the system when bonds are broken.

Initial conditions.–

Basics.–

Before applying the pressure, one builds the system by adding N particles in the box. We use standard reaction-limited cluster-cluster aggregation (RCCA) model [15] to generate randomly aggregates. This model is known to correctly describe experimental flocculation of colloidal particles – such as silica [16], polystyrene [17], or metallic [18] colloids – in the conditions where the aggregation rate is limited by the time it takes by the clusters to form a bond. The model generates an ensemble of disordered fractal aggregates, of fractal dimension $D_f = 2.1$.

Once an aggregate is generated, it is inserted randomly at top of the box. The aggregate is then gently settled onto bottom of the box, or onto existing particles, without deformation of its structure nor overlap.

Any alternative pre-aggregation process can be used as well. One important issue is to know if the proper sizes of the initial aggregates may play a role in the compaction process. Indeed, the size of the initial fractal clusters defines a correlation length in the system, what can be quite important for the subsequent collective deplacement of the particles. This question is yet unsolved.

Below, we discuss an example (flow around fixed obstacle) where pre-aggregation is not considered, all the particles being placed randomly at the beginning, with a definite volume fraction.

HOMOGENEOUS COMPRESSION

Results of the numerical model.–

A sketch of the visual aspect of the particle system (bonds are not represented) is shown in Fig.2 for three different pressures. these are projections onto a plane, so the system appears more dense than it actually is. One can note that, except for small statistical fluctuations, the systems appear to be spatially homogeneous. This result – which can be made more quantitative by a study of the average volume fraction through slabs [11] –, is well known in compression experiments [19].

Double-logarithmic plot for the external pressure versus the volume fraction of the particles is shown in Fig.3. Several sets of data are represented, all of them obtained from numerical simulations of systems with $\simeq 500$ particles, 200 pins per particle. Four sets of values of E_d are shown, namely $E_d/E_o = 0.04, 4, 9$, and in the range $360 \sim 10000$. The latter case corresponds to rupture lengths comparable to the box size.

Two power-law behaviors

$$P/P_o \propto \phi^\delta \ , \tag{4}$$

are clear on the Fig.3. One with a slope $\delta \simeq 4.4$ will be called elastic as it corresponds to small amount of bond breaks. This is *not* exactly elastic behavior because bonds are created through compression advancement, but the created bonds are essentially permanent at this stage. The other exponent is $\delta \simeq 1.7$, and is recovered in the mid-range of values of the volume fraction, namely $0.07 < \phi < 0.5$, for any value of the disruptive energy E_d larger than E_o. This corresponds to plastic behavior as the rate of creation-destruction process for the bonds, is maximum [11].

An important point to notice here is that the equations (4) are constitutive equations dependent only on the material [11]. Particularly, they do not depend, in the statistical sense, on the initial conditions, on the pres-
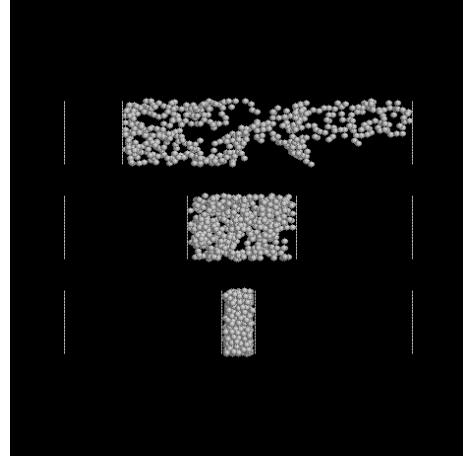

FIGURE 2. Three pictures (projection) of the same system during compaction under uniform pressure. The value of E_d/E_o is here equal to 4, and the total number of particles is 500. Volume fraction are respectively 0.06, 0.30 and 0.63 from top to bottom. The dashed lines visualize the initial and actual planes where external pressure is applied. Periodic boundary conditions are used on all other sides.

sure increment (if small enough) or on the periodic or fixed boundary conditions (if the system is large enough). Even the proper values of some parameters, such as the number of pins per particle (provided it is large enough), or the polydispersity of the particle radius (if narrow), are not relevant. Such universality allows direct comparison between results of the numerical simulations and experimental data on compression of colloidal pastes. This was done successfully in recent works [19, 20, 21].

Theoretical arguments.–

The elastic behavior.–

When bond breaking is unlikely to occur (at the very beginning of the compression process or because of the large value of the disruptive energy), the system behaves as a disordered elastic network. The response of the system is due to the presence of resistant columns whose structure is a consequence of the initial fractal morphology of the individual aggregates. Given a homogeneous arrangement of such disordered fractal aggregates, the overall elastic modulus K, of the system, writes [22] :

$$K \propto \phi^{(3+x)/(3-D_f)} \ , \tag{5}$$

with the fractal dimension of the backbone of the individual clusters $x \simeq 1.4$. This leads to $\delta \simeq 4.8$ in (4). Alternative derivations were proposed [23], leading to values of exponent δ in between 4 and 5. Precise analysis of the
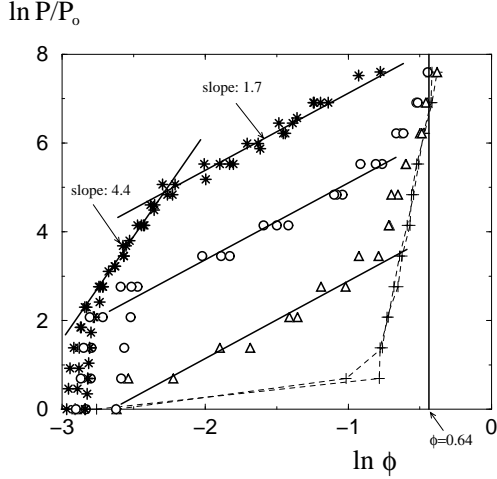
FIGURE 3. Double-logarithmic plot of the reduced pressure P/P_o vs the volume fraction ϕ for various values of the disruptive energy, E_d : $E_d/E_o = 4$ (triangles), $E_d/E_o = 9$ (circles) and various values of E_d/E_o above 360 (stars). A dashed line is used for the smallest values of E_d (namely $E_d/E_o = 0.04$), which exhibits fragile behavior as discontinuous jumps in ϕ from 0.01 to 0.5 at $P/P_o \simeq 1.3$. Full lines are the power-law behaviors (4) with exponents 4.4 and 1.7 for the elastic and plastic behaviors respectively.

theoretical arguments, with comparison with the numerical simulations, remains to be done.

The plastic behavior.–

Rupture of the resistant columns occur if the applied pressure is larger than the threshold $P^\star$ for which the density of elastic energy stored in a column becomes equal to the average energy needed to break up all the bonds linking two neighboring particles of the column [24]. The latter energy is independent on the volume fraction, then $P^\star \propto \sqrt{K}$ with a proportionality constant independent on ϕ. On the other hand, the effective stiffness of a disordered column is [25] : $K = nka/N_r R_\perp^2$, with $N_r \sim H^{d_{min}}$ the number of particles involved in the minimal chain throughout a percolating system of overall size H (and $d_{min} \simeq 1.4$ [26]). The distance $R_\perp$ follows a simple power-law $R_\perp \propto H$ for the isotropic chains [27]. This results in the power-law dependence of the critical pressure $P^\star$ with the volume fraction as :

$$P^\star \propto \phi^{1+d_{min}/2} . \tag{6}$$

Interpretation of (6) in terms of the current pressure P, can be done by the following argument [28]. When P reaches the threshold $P^\star(\phi)$ corresponding to the actual volume fraction through (6), then the resistant column of height H breaks into two or more fragments, and
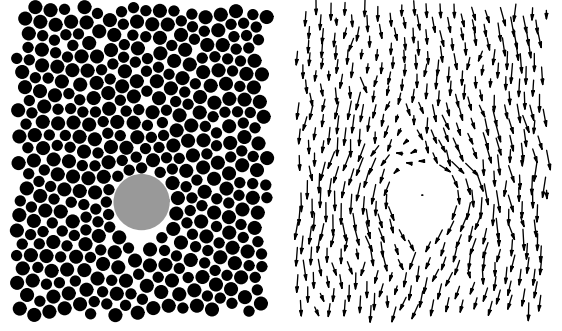

FIGURE 4. Central part of a 2-dimensional colloidal dispersion flowing around an intruder in a box with periodic boundary conditions. The flow goes regularly from top to bottom and the intruder is fixed. Two sizes of particles are used in order to avoid cristallization. On the left, location of the particles (drawn as black circles) at a given time of the stationary state. The bonds between particles are not drawn. The still intruder is the large grey circle. On the right, instantaneous velocity of the particles for the same system as on the left.

the volume fraction ϕ increases by elastic deformation of the next resistant column. As this process goes on, the system passes through a series of discrete states $(P^\star(\phi), \phi)$. If the disordered system is large enough, the states $(P^\star(\phi), \phi)$ are close to each other, and :

$$P \propto \phi^{1+d_{min}/2} , \tag{7}$$

is then expected, with the exponent $1 + d_{min}/2 \approx 1.7$.

FLOW AROUND OBSTACLE

We present here another experimental situation related to the same problematics. Let us consider a colloidal dispersion confined in between two glass plates. The paste is flowing because of a pressure gradient, and a fixed intruder (here, a disk) is placed in the center of the system. This geometry was recently studied in details for the granular matter [29]. The particles are put randomly at the beginning of the experiments (real or numerical).

Contrary to the pure granular matter, short-range attractive interactions exist now between the sticky particles. This induces strong correlations in the fluid, which can be seen on Fig.4. In particular, the proper size of the void created downstream after the intruder depends essentially on the properties of the non-permanent microscopic springs. The average flow pattern is another example of a macroscopic field depending on the microscopic properties of the material.

CONCLUSION

We presented in this paper a numerical model of sticky granular systems, based on simple physical features, working with a limited number of parameters. The model allows realistic approach of the static and dynamic behaviors of these complex collective systems – generically called pastes –, which exhibit plastic behavior and non-linear response to mechanical stress. This numerical tool allows to study in details the close relationship between the microscopic interactions and macroscopic deformation or flow of a paste.

During compression of a colloidal dispersion, two stages are clear and related to particular scaling laws. In the first one, very few interparticle bonds are broken. Displacement of colloidal aggregates within the structure lead to the collapse of the largest voids, while the smallest voids and the local structure remain unchanged. In the second stage, the compression causes the rupture of bonds everywhere in the system and the collapse of voids of any size. As a result, the less-dense regions of the aggregates are compressed, and they form a homogeneous dispersion. Meanwhile, the denser cores of the aggregates are pushed through this soft material, collect more particles, and turn into dense space-filling lumps.

During flow of a paste, the interparticle bonds generate strong correlation effects in the Non-newtonian complex fluid, resulting in self-organized structures such as large voids around obstacles.

ACKNOWLEDGMENTS

REFERENCES

1. R.G. Gillies and C.A. Shook *Canad. J. Chem. Eng.*, **78**, 709–716 (2000).
2. Z. Saada, J. Canou, L. Dormieux, J.C. Dupla, and S. Maghous *Int. J. Numer. Anal. Methods Geomech.*, **29**, 691-711 (2005).
3. H. Kimura, Y. Nakayama, A. Tsuchida and T. Okubo, *Colloids and Surface B: Biointerfaces*,textbf 56, 236–240 (2007).
4. K. Holmberg *Handbook of Applied Surface and Colloid Chemistry*, vol.1, John Wiley and sons Inc., New York, 2001.
5. P. Coussot *Rheometry of Pastes, Suspensions, and Granular Materials: Applications in Industry and Environment*, John Wiley and sons Inc., Hoboken, 2005.
6. T.C. Halsey and A.J. Levine *Phys. Rev. Lett.* **8**0, 3141–3144 (1998).
7. S.L. Diamond, *Biophys. J.* **8**0, 1031–1032 (2001).
8. S. Herminghaus *Advances in Physics* **5**4, 221–244 (2005).
9. R. Buscall, P.D.A. Mills, R.F. Stewart, D. Sutton, L.R. White and G.E. Yates *J. Non-Newtonian Fluid Mech.* **2**4 183–202 (1987).
10. S. Feng, P.N. Sen, B.I.Halperin and C.J. Lobb, *Phys. Rev. B* **3**0 5386–5389 (1984).
11. R. Botet and B. Cabane, *Phys. Rev. E* **7**0, 031403-1–11 (2004).
12. C. Allain and L. Limat, *Phys. Rev. Lett.* **7**4, 2981–2984 (1995).
13. P.A. Cundall and O.D.L. Strack, *Geotechnique* **2**9 47-65 (1979).
14. D.C. Rapaport, *The art of molecular dynamics simulation*, 2nd edition, Cambridge University Press, 2004.
15. R. Jullien and R. Botet, *Aggregates and Fractal Aggregates*, World Scientific, Singapore, 1987.
16. Z. Zhou and B. Chu, *J. Colloid Interface Sci.* **1**46, 541–555 (1991).
17. V. Oles, *J. Colloid Interface Sci.* **1**54, 351–358 (1992).
18. D.A. Weitz, J.S. Huang, M.Y. Lin and J. Sung, *Phys. Rev. Lett.* **5**4, 1416–1419 (1985).
19. J.B. Madeline, M. Meireles, C. Bourgerette, R. Botet, R. Schweins and B. Cabane, *Langmuir* **2**3, 1645–1658 (2007).
20. J.B. Madeline, M. Meireles, J. Persello, C. Martin, R. Botet, R. Schweins and B. Cabane, *Pure Appl. Chem.* **7**7 1369–1394 (2005).
21. C. Parneix, *Agrégats colloïdaux destinés au renforcement des élastomères*, PhD thesis, Université de Franche-Comté, Besançon, France (2006).
22. W.D. Brown and R.C. Ball, *J. Phys. A* **1**8, L517–L521 (1985).
23. R. Buscall, P.D.A. Mills, J.W. Goodwin, D.W.J. Lawson, *Chem. Soc. Faraday Trans* 1 **8**4, 4249–4260 (1988);
Wei-Heng Shih, Wan Y. Shih, Seong-Il Kim, Jun Liu and Ilhan A. Aksay, *Phys. Rev. A* **4**2, 4772–4776 (1990);
M. Chen, W.B. Russell, *J. Colloid Interface Sci.* **1**41, 564–577 (1991);
Hua Wu and M. Morbidelli, *Langmuir* **1**7, 1030–1036 (2001).
24. S.O. Gregg *The Surface Chemistry of Solids*, Chapman and Hall, London, 1965.
25. Y. Kantor and I. Webman, *Phys. Rev. Lett.* **5**2, 1891–1894 (1984).
26. J. Vannimenus, in *Physics of Finely Divided Matter*, N. Boccara and M. Daoud eds, Springer-verlag, Proc. in Physics 5, Berlin, 1985, p. 317.
27. A.A. Potanin, *J. Colloid Interface Sci.* **1**57, 399–410 (1993) ;
A.A. Potanin and W.B. Russel, *Phys. Rev. E* **5**3, 3702–3709 (1996).
28. R. Buscall and L.R. White, *J. Chem. Soc. Faraday Trans.* I **8**3, 873–891 (1987).
29. E. Kolb, J. Cviklinski, J. Lanuza, P. Claudin, and E. Clément, *Phys. Rev. E* **6**9, 0313006-1–5 (2004).